

Document downloaded from:

<http://hdl.handle.net/10251/60407>

This paper must be cited as:

Llopis Albert, C.; Palacios Marqués, D.; Merigó, JM. (2014). A coupled stochastic inverse-management framework for dealing with nonpoint agriculture pollution under groundwater parameter uncertainty. *Journal of Hydrology*. 511:10-16. doi:10.1016/j.jhydrol.2014.01.021.



The final publication is available at

<http://dx.doi.org/10.1016/j.jhydrol.2014.01.021>

Copyright Elsevier

Additional Information

1 **A coupled stochastic inverse-management framework for dealing with nonpoint**
2 **agriculture pollution under groundwater parameter uncertainty**

3

4 Llopis-Albert, Carlos^a; Palacios-Marques, D.^b; Merigó, J.M.^c

5

6 ^a Universitat Politècnica de València, Camí de Vera s/n, Spain, 46022; email: cllopisa@gmail.com

7 ^b Universitat Politècnica de València, Camí de Vera s/n, Spain, 46022, email: dapamar@doe.upv.es

8 ^c University of Manchester, Booth Street West, M15 6PB Manchester, United Kingdom, email:

9 jose.merigolindahl@mbs.ac.uk

10

11 **Abstract**

12 In this paper a methodology for the stochastic management of groundwater quality
13 problems is presented, which can be used to provide agricultural advisory services. A
14 stochastic algorithm to solve the coupled flow and mass transport inverse problem is
15 combined with a stochastic management approach to develop methods for integrating
16 uncertainty; thus obtaining more reliable policies on groundwater nitrate pollution
17 control from agriculture. The stochastic inverse model allows identifying non-Gaussian
18 parameters and reducing uncertainty in heterogeneous aquifers by constraining
19 stochastic simulations to data. The management model determines the spatial and
20 temporal distribution of fertilizer application rates that maximizes net benefits in
21 agriculture constrained by quality requirements in groundwater at various control sites.
22 The quality constraints can be taken, for instance, by those given by water laws such as
23 the EU Water Framework Directive (WFD). Furthermore, the methodology allows
24 providing the trade-off between higher economic returns and reliability in meeting the

25 environmental standards. Therefore, this new technology can help stakeholders in the
26 decision-making process under an uncertainty environment. The methodology has been
27 successfully applied to a 2D synthetic aquifer, where an uncertainty assessment has
28 been carried out by means of Monte Carlo simulation techniques.

29

30 **Keywords:** Stochastic inversion; Gradual deformation; Non-Gaussian; Nitrate pollution;
31 Fertilizer standards; Optimization

32

33 **1. Introduction**

34 Groundwater is the ultimate source of freshwater to sustain many important agricultural
35 production areas when surface water sources have been depleted. Furthermore,
36 irrigation is the most important water use accounting for about 70% of the global
37 freshwater withdrawals and 90% of consumptive water uses. Although the development
38 of an intensive agriculture represents one of the main factors in the current economic
39 development of many regions, it has also become an important environmental issue in
40 recent years. This is because it poses many impacts and threats to groundwater bodies,
41 such as overdrafting, aquifer pollution, impacts on downstream demands or impacts on
42 Groundwater Dependent Ecosystems (GDEs). Water laws and policies around the world
43 try to deal with such problems. For instance, the EU Water Framework Directive (EC,
44 2000) stipulates that groundwater bodies must achieve a good chemical and quantitative
45 status by a set deadline.

46 However, the decision-making process in groundwater management protection is
47 complex because of heterogeneous stakeholder interests, multiple objectives, key
48 drivers influencing the agricultural market and farmer's decisions, land-use/crop pattern
49 evolution and uncertain outcomes. A wide range of stakeholders play an active role in

50 water resources management. They range from irrigation communities, government,
51 river basin authority, Non Governmental Organisations (NGO's), agri-business
52 industries, farmers to electric power industries (because of groundwater abstraction
53 costs). Moreover, integrated water resources management incorporates technical,
54 scientific, political, legislative and organizational aspects of a water system. Because of
55 that, stakeholders need new technologies and tools to help them in the decision-making
56 process. This links with the main goal of this paper, which is to present a hydro-
57 economic modeling framework for agricultural advisory services. Specifically, this
58 work is intended to analyze the influence of uncertainty in the physical parameters of a
59 heterogeneous groundwater diffuse pollution problem on the results of management
60 strategies, and to introduce methods that integrate uncertainty and reliability in order to
61 obtain strategies of spatial allocation of fertilizer use in agriculture.

62 The methodology is based on the coupling of a stochastic inverse model to identify non-
63 Gaussian parameters and to reduce uncertainty in heterogeneous aquifers with a
64 groundwater quality management model for dealing with non-point agriculture
65 pollution. It should be mentioned that a small number of papers in the literature have
66 developed a similar approach as that here presented (e.g., Bark el al., 2003).

67 The stochastic inverse model allows identifying non-Gaussian parameters and reducing
68 uncertainty in flow and mass transport predictions by constraining stochastic
69 simulations to data, while the optimization management model determines the spatial
70 and temporal distribution of fertilizer application rates that maximizes net benefits in
71 agriculture constrained by quality requirements in groundwater at various control sites.

72 Inverse modelling has become an important and necessary step in hydrogeological
73 studies (e.g., Poeter and Hill, 1997). This is because the inability to characterize aquifer
74 heterogeneity properly, which makes predictions of contaminant concentration highly

75 uncertain. Consequently, the predictions of management models based on groundwater
76 quality standards are also uncertain. The literature on groundwater inverse modelling
77 mostly focuses on the estimation of parameters and its underlying uncertainty. This is
78 because they are the most relevant factors affecting mass transport predictions (Smith
79 and Schwartz, 1981) and because conceptual uncertainties are difficult to be formalized
80 in a rigorous mathematical framework (Renard, 2007). Regarding the different
81 groundwater parameters we have focused on the hydraulic conductivity, owing to the
82 fact that it is the paramount parameter controlling the flow and solute transport in
83 groundwater. In fact, it can vary spatially by several orders of magnitude. For instance,
84 the aquifer at the Columbus Air Force Base in Mississippi, commonly known as the
85 Macrodispersion Experiment (MADE) site, is a strongly heterogeneous system with a
86 variance of the natural logarithm of K of nearly 4.5 (e.g., Rehfeldt et al., 1992).
87 Eventually, once the groundwater parameter uncertainty has been strongly reduced by
88 the inverse model, more reliable policies can be defined using the hydro-economic
89 model. It explicitly integrates nitrate leaching and fate and transport in groundwater
90 with the economic impacts of nitrogen fertilizer restrictions in agriculture.
91 The remaining of the paper is organized as follows: firstly, a background of the
92 stochastic inverse model and the management model is presented; secondly, the
93 methodology has been verified on a 2D synthetic case. Finally, we have highlighted the
94 advantages of using the methodology for providing agricultural advisory services to
95 policy-makers.

96

97 **2. Modeling framework**

98 The methodology is based on the coupling of a stochastic inverse model to identify non-
99 Gaussian parameters and to reduce uncertainty in heterogeneous aquifers with a

100 groundwater quality management model for dealing with non-point agriculture
101 pollution. An explanation of both models is provided below:

102

103 **2.1. Stochastic inverse model (the GC method)**

104 The GC method is a stochastic inverse modeling technique for the simulation of
105 conductivity (K) fields in aquifers which has been developed to overcome several of the
106 limitations found in the already existing techniques (Llopis-Albert, 2008; Capilla and
107 Llopis-Albert, 2009). The method was exhaustively verified on a 2D synthetic aquifer
108 (Llopis-Albert and Capilla, 2009). In addition, a 3D application to the Macrodispersion
109 Experiment (MADE-2) site, on a highly heterogeneous aquifer at Columbus Air Force
110 Base in Mississippi (USA) was presented by Llopis-Albert and Capilla (2009a); and
111 also on a complex real-world case study in a fractured rock site (Llopis-Albert and
112 Capilla, 2010). Furthermore, it was extended to deal with independent stochastic
113 structures belonging to independent K statistical populations (SP) of fracture families
114 and the rock matrix, each one with its own statistical properties (Llopis-Albert and
115 Capilla, 2010a).

116 The method uses an iterative optimization procedure to simulate K fields honoring K
117 measurements, secondary information obtained from expert judgment or geophysical
118 surveys, transient piezometric head (h) data and concentration (c) measurements. Travel
119 time data can also be considered by means of a backward-in-time probabilistic model
120 (Neupauer and Wilson, 1999), which extends the applications of the method to the
121 characterization of sources of groundwater contamination. The formulation of the
122 method does not require assuming the classical multi-Gaussian hypothesis allowing the
123 reproduction of strings of extreme values of K that often take place in nature, being
124 these formation features crucial in order to obtain realistic and safe estimations of mass

125 transport predictions. The method has been developed using a modified version of the
126 gradual deformation technique (Hu, 2000), and applying a Lagrangian approach to solve
127 the mass transport equation. This allows avoiding numerical dispersion usually found in
128 Eulerian approaches. The algorithm has been implemented for 3D transient flow
129 problems under variable density flow conditions, considering the dispersion as a
130 tensorial magnitude, and a first-order mass transfer approach. Performing a Bernoulli
131 trial on the appropriate phase transition probabilities, the particle distribution between
132 the mobile domain and the immobile domain can be determined (Salamon et al., 2006).
133 The iterative optimization process for constraining stochastic simulations to data is
134 carried out by doing non-linear combinations of seed conditional realizations. These
135 seed conductivity (K) fields are already conditional to K and secondary data, and are
136 generated by sequential indicator simulation. The a priori stochastic structure of these K
137 seed fields is defined by means of the local conditional cumulative density functions
138 (ccdf's) and the indicator variograms, thus allowing the GC method to adopt any
139 Random Function (RF) model. As a first step, the GC method builds linear sequential
140 combinations of non multiGaussian K fields that honour K data:

$$141 \quad K^m = \alpha_1 K^{m-1} + \alpha_2 K_{2m} + \alpha_3 K_{2m+1} \quad \text{with} \quad K^0 = K_1 \quad (1)$$

142 where subscripts stand for seed fields and superscripts for conditional fields resulting
143 from a previous linear combination. That is, at m iteration, the field K^{m-1} , from the
144 previous iteration, is combined with two new independent realizations K_{2m} and K_{2m+1} .
145 The procedure requires combining at least three conditional realizations at a time to
146 ensure the preservation of mean, variance, variogram and K data in the linearly
147 combined field. The coefficients have also to fulfill the constraints in Eq. (2):

$$148 \quad \begin{cases} \alpha_1 + \alpha_2 + \alpha_3 = 1 \\ (\alpha_1)^2 + (\alpha_2)^2 + (\alpha_3)^2 = 1 \end{cases} \quad (2)$$

149 being the parameterization of α_i given by Eq. (3):

$$150 \quad \begin{cases} \alpha_1 = \frac{1}{3} + \frac{2}{3} \cos \theta \\ \alpha_2 = \frac{1}{3} + \frac{2}{3} \sin(-\frac{\pi}{6} + \theta) \\ \alpha_3 = \frac{1}{3} + \frac{2}{3} \sin(-\frac{\pi}{6} - \theta) \end{cases} \quad \text{with } \theta \in [-\pi, \pi] \quad (3)$$

151

152 The α_i coefficients are different in every iteration m , and correspond to a unique
153 parameter θ ; note the one to one correspondence between the parameter and the
154 combined realization K^m .

155 Because the linear combination of independent non-Gaussian random functions does
156 not preserve the non-Gaussian distribution, although the variogram is preserved, a
157 transformation between Gaussian to the non-Gaussian fields (and vice versa) is
158 required. This transformation is performed through the probability fields (see Capilla
159 and Llopis-Albert 2009 for more details). Finally, at each iteration m of the method the
160 parameter θ is determined by minimizing an objective function that penalizes deviations
161 among computed and measured data. As aforementioned this way of operating has been
162 successfully applied in both synthetic and real cases.

163 The penalty function to be minimized is made up by the weighted sum of three terms:

$$164 \quad p^k(\theta) = p_h^k(\theta) + \Phi^k p_c^k(\theta) + \Psi^k p_t^k(\theta) \quad (4)$$

165

166 where $p_h^k(\theta)$ is the weighted sum of square differences between observed and
167 calculated values for piezometric heads, concentrations and travel times, respectively.
168 These terms are function of the parameter θ , for every time step t and measurement
169 location i . The terms Φ^k and Ψ^k are trade-offs coefficients between the different
170 conditioning data (see Capilla and Llopis-Albert, 2009).

171

172 2.2. Hydro-economic model

173 The method is based on previous developments of the hydro-economic modeling
174 framework presented by Peña-Haro et al. (2009; 2011). The model was also applied to a
175 real-complex case study (Peña-Haro et al., 2010) and further extended to assess
176 different sources of uncertainty on the suggested control policies and the resulting
177 economic and environmental impacts (Llopis-Albert et al., 2014).

178 The stochastic optimization approach determines the spatial and temporal fertilizer
179 application rate that maximizes the net benefits in agriculture constrained by the quality
180 requirements in groundwater at various control sites. It quantifies the relationship
181 between emissions (fertilizer applied) and groundwater quality impacts or nitrate
182 concentration measured at regulatory control sites. The regulation of nitrate pollution is
183 examined within a cost-effectiveness way, in which the objective is to maximize the
184 sum of the net benefits from agricultural production while meeting the environmental
185 standards. The management model for groundwater pollution control is formulated as
186 follows, where the benefits in agriculture are determined by means of crop prices and
187 crop production functions:

$$188 \quad Max \Pi = \sum_s \sum_y \frac{1}{(1+r)^y} A_s (p_s \cdot Y_{s,y} - p_n \cdot N_{s,y} - p_w \cdot W_{s,y} - C_s + S_s) \quad (5)$$

189 subject to:

$$190 \quad \sum_s \mathbf{RM}_{c,t \times s,y} \cdot \mathbf{cr}_{s,y} \leq \mathbf{q}_{c,t} \quad \forall c, t, y \quad (6)$$

191 where Π is the objective function to be maximized and represents the present value of
192 the net benefit from agricultural production (€) defined as crop revenues minus fertilizer
193 and water variable costs; A_s is the area cultivated for crop located at source s ; p_s is the
194 crop price (€/kg); $Y_{s,y}$ is the production yield of crop located at source s at planning year

195 y (kg/ha), that depends on the nitrogen fertilizer and irrigation water applied; p_n is the
196 nitrogen price (€/kg); $N_{s,y}$ is the fertilizer applied to crop located at source s at year y
197 (kg/ha), p_w is the price of water (€/m³), and $W_{s,y}$ is the water applied to crop located at
198 source s at each planning year y (m³); C_s is the aggregation of the remaining per hectare
199 cost for crop located at source s (€/ha); S_s are the subsidies for the crop located at
200 source s (€/ha); r is the annual discount rate, \mathbf{RM} is the unitary pollutant concentration
201 response matrix where each column is the nitrate concentration for each crop area (s)
202 times de number of years within the planning horizon (y), the number of rows equals the
203 number of control sites (c) times the number of simulated time steps (t) in the frame of
204 the problem; \mathbf{q} is a vector of water quality standard imposed at the control sites over the
205 simulation time (kg/m³); \mathbf{c}_r is a vector representing the nitrate concentration recharge
206 (kg/m³) reaching groundwater from a crop located at source s , which is obtained
207 dividing the nitrate leached over the water that recharges the aquifer. C_s is the
208 aggregation of the remaining per hectare costs for crop located at sources (€/ha); S_s are
209 the subsidies for the crop located at source s (€/ha).

210 The response matrix (\mathbf{RM}) describes the influence of pollutant sources upon
211 concentrations at the control sites over time. This is carried out by means of numerical
212 simulation models based on the flow and solute transport governing equations.
213 Specifically, in order to ensemble the pollutant response matrix we have used
214 MODFLOW (McDonald and Harbough, 1988), a 3D finite difference groundwater flow
215 model, and MT3DMS (Zheng and Wang, 1999), a 3D solute transport model. The
216 hydro-economic framework takes into account different processes governing nitrate in
217 groundwater in both the saturated and unsaturated zone of the aquifer. Then the
218 agronomic, and the flow and solute transport model consider processes ranging from
219 mineralization, nitrification, denitrification, volatilization, immobilization, and plant

220 uptake in the unsaturated zone to advection, dispersion, diffusion and biodegradation in
221 the saturated zone.

222 The simulated time horizon corresponds to the time for the solute to pass all the control
223 sites, and it is independent of the length of the planning period. Once the field of
224 groundwater velocities is computed using the calibrated groundwater flow model, it is
225 used by the calibrated mass transport model to compute the nitrate concentrations over
226 time each control site (breakthrough curves) at resulting from unit nitrate concentration
227 recharges at each pollution source. These concentration values are assembled as
228 columns to conform the pollutant concentration ***RM***, which is a rectangular ($m \times n$)
229 matrix. The number of columns, n , equals the number of crop areas (pollution sources)
230 times the number of years within the planning horizon. The number of rows, m , equals
231 the number of control sites times the number of simulated time steps in the frame of the
232 problem. The integration of the response matrix in the constraints of the management
233 model allows simulating by superposition the evolution of groundwater nitrate
234 concentration over time at different points of interest throughout the aquifer resulting
235 from multiple pollutant sources distributed over time and space. The assumption of
236 linearity of the system is required in order to apply superposition. The advective and
237 dispersive transport depends on concentration and groundwater flow velocity. Because
238 concentration is unknown, the use of both velocity and concentration as decision
239 variables would create a non-linearity. As a result the underlying assumption is that the
240 irrigation rate at each source is not a decision variable and has a known influence upon
241 the velocity field.

242 Both nitrate leached and crop production are represented by polynomial regression
243 equations depending on the water and fertilizer use (Peña-Haro et al., 2009). These
244 equations are derived from the results of the agronomic simulation model GEPIC (Liu

245 et al., 2007), a GIS-based crop growth model integrating a bio-physical EPIC model
 246 (Environmental Policy Integrated Climate) (Williams, 1995) with a GIS to simulate the
 247 spatial and temporal dynamics of the major processes of the soil-crop-atmosphere-
 248 management systems. The GEPIC package simulates crop growth using local conditions
 249 on climate, soil, irrigation water, tillage and other operations. The crop production
 250 function was introduced into the management model as follows:

251

$$Y_{s,y} = a + b \cdot W_{s,y} + c \cdot W_{s,y}^2 + d \cdot N_{s,y} + e \cdot N_{s,y}^2 + f \cdot W_{s,y} \cdot N_{s,y} \quad (7)$$

253

254 where $Y_{s,y}$ is the crop yield located at source s for a year y (kg/ha), $W_{s,y}$ is the water
 255 applied to the crop located at source s (m^3 /ha) and $N_{s,y}$ is the fertilizer applied to the
 256 crop located at source s (kg/ha) within the year y . The nitrogen leached is defined as
 257 follows:

258

$$L_{s,y} = g + h \cdot W_{s,y} + i \cdot W_{s,y}^2 + j \cdot N_{s,y} + k \cdot N_{s,y}^2 + l \cdot W_{s,y} \cdot N_{s,y} \quad (8)$$

260

261 where $L_{s,y}$ is the nitrogen leached (kg/ha), $W_{s,y}$ is the water applied to the crop located at
 262 source s (m^3 /ha) with in the year y , and $N_{s,y}$ is the fertilizer applied to the crop located at
 263 source s (kg/ha).

264 The non-linear optimization problem was coded in GAMS, a high-level modeling
 265 system for mathematical programming problems (GAMS, 2012), while the solver used
 266 was CONOPT (Drud, 1985). It is based on the Generalized Reduced Gradient algorithm
 267 designed for large programming problems.

268

269 **3. Application to a 2D synthetic case**

270 A two-dimensional synthetic aquifer was selected to verify the methodology. It is based
271 on the configuration presented by Peña-Haro et al. (2009), which apply a deterministic
272 formulation to a 2D homogeneous synthetic aquifer. In this case, however, we consider
273 heterogeneous hydraulic conductivity. The aquifer has impermeable boundaries and
274 steady-state flow from top to bottom of the domain (Fig. 1). The aquifer domain was
275 divided in square cells of 500 x 500 m, with a grid made up of 58 rows and 40 columns.
276 A confined aquifer has been modeled with a saturated thickness of 10 m, effective
277 porosity of 0.2, and longitudinal dispersivity of 10 m. The natural annual recharge is
278 $500 \text{ m}^3/\text{ha}$. A temporal discretization of 70 stress periods was used, each of one-year
279 duration. In addition, seven different crop areas (which are the pollution sources in our
280 model formulation) with five different crops are considered. For each crop a quadratic
281 production function and a leaching function have been defined using Eq. (7) and (8).
282 The calibrated coefficients of those quadratic functions can be found in Peña-Haro et al.
283 (2009). The relationship between each source and the crop sown is depicted in Table 1,
284 which also shows the irrigation rates needed by each crop. A recovery time horizon of
285 the aquifer by the year 2015 is defined, which entails nitrate concentration lower than
286 50 mg/l for all control sites (three control wells are defined), as established by the EU
287 water legislation.

288 Two scenarios have been simulated in order to compare the groundwater nitrate
289 concentrations and net profits. In scenario 1 (S1) the fertilizer use is not constrained by
290 groundwater nitrate concentration standards at the control wells. It represents the
291 fertilizer application rates that return the maximum net benefits at each crop.

292 In scenario 2 (S2) the fertilizer used is constrained by the groundwater nitrate
293 concentration standards (50 mg/l) at the control wells. Finally, a planning horizon of

294 forty years was considered for each scenario with a constant annual fertilizer application
295 for the whole time period.

296 An ensemble of a hundred conditional seed K fields is generated by means of sequential
297 indicator simulation (SIS) by means of the code ISIM3D (Gómez-Hernández and
298 Srivastava, 1990). The conditional fields represent the Case 1 (C1). In addition, an
299 ensemble of unconditional K fields has also been generated in order to compare results
300 (Case 2, C2). This geostatistical tool allows controlling the bivariate (2-point) statistics
301 imposed on the simulated field instead of controlling a mere covariance model. As
302 aforementioned, these seed K fields are subsequently used by the inverse model to
303 constraint stochastic simulations to the available data. It should be mentioned that all
304 seed K fields honour the K data, while during the stochastic optimization procedure
305 carried out by the inverse model, the K fields are gradually modified to honour the flow
306 and mass transport data. Eighty-four K data were defined as conditioning data. They
307 have been selected to be homogeneously and spatially distributed over the whole aquifer
308 domain. Moreover, they differ in several orders of magnitude to obtain highly
309 heterogeneous aquifers. With the information provided by the K data we have defined
310 nine deciles of the cumulative distribution to give a reasonable discretization of the
311 local distribution and transformed to the corresponding indicator categories. The SIS
312 uses an indicator kriging (Deutsch and Journal, 1997) to build up a discrete conditional
313 cumulative density function (ccdf) for the individual categories at each case and the
314 node is assigned a category selected at random from this discrete ccdf. For a continuous
315 variable such as conductivity, indicator variables are built by comparing data values to a
316 set of thresholds, z_k :

$$317 \quad i(\mathbf{u}_\alpha; k) = \begin{cases} 1 & \text{if } z(\mathbf{u}_\alpha) \leq z_k \\ 0 & \text{otherwise} \end{cases} \quad (9)$$

318 Spatial continuity for the different thresholds was then evaluated using the standardized
 319 indicator semivariogram (e.g., Goovaerts, 1997):

$$320 \frac{\gamma_I(\mathbf{h}; z_k)}{\sigma_i^2} \approx \frac{1}{2N(\mathbf{h})} \sum_{\mathbf{u}_1 - \mathbf{u}_2 = \mathbf{h} \pm \Delta \mathbf{h}} [i(\mathbf{u}_1; z_k) - i(\mathbf{u}_2; z_k)]^2 \quad (10)$$

321

322 where z_k are the thresholds values; σ_i^2 is the indicator variance given as $\sigma_i^2 =$
 323 $F(z_k)[1 - F(z_k)]$, and $F(z_k)$ is the marginal cumulative distribution function; $N(\mathbf{h})$ is
 324 the number of data pairs within the class of distance and direction; \mathbf{h} is the separation
 325 vector; $z(\mathbf{u}_{1,2})$ denotes a measurement with $\mathbf{u}_{1,2}$ being the vector of spatial coordinates of
 326 the individual 1 or 2; and $\Delta \mathbf{h}$ is a tolerance vector. Finally, a mosaic variography was
 327 chosen for the generation of the seed K fields with the defined spatial continuity. It is
 328 spherical, with equal ranges in all directions of 40 m, 0.04 of nugget effect, and sill of
 329 0.22. The generated seed fields are equally likely realizations, thus being plausible
 330 representations of reality since they display the same degree of spatial variability.

331 Note that we have focused in order to generate the heterogeneous fields on the hydraulic
 332 conductivity (K), since it is usually the parameter with the most significant spatial
 333 variation. One of these seed K fields has been chosen to be the true K field (i.e., it
 334 represents the actual heterogeneity in the aquifer). For the true field the hydraulic heads
 335 (h) are obtained and used as conditioning data for the inverse model. The spatial
 336 location of the 84 piezometric head data is the same than those defined for the K data.

337 The a priori conditional cumulative density function (ccdf) have been defined
 338 displaying a highly asymmetrical distribution with a long lower tail; thus assigning
 339 higher probabilities of occurrence to high K values (i.e., it could represent fracture
 340 structures). This is how the GC method allows integrating the available hard data and
 341 also the geological information. Note that GC method honors the a priori ccdf's during
 342 the whole conditioning process, while other inverse modeling techniques deal with

343 secondary information incorporating it in initially generated fields to be perturbed, not
344 having any implemented constraint to keep honoring these data. Furthermore, GC
345 method tends to preserve the local ccdf's during the whole perturbation process of seed
346 K fields to obtain conditional simulations see Llopis-Albert and Capilla (2009). This
347 means that if there are zones with ccdf's belonging to independent stochastic processes
348 they are still preserved. In addition, conductivities can vary, due to the deformation
349 process, several orders of magnitude, and because of how the non-Gaussian feature is
350 introduced in the inverse model by means of the probability fields allows the
351 reproduction of strings of extreme values of K or preferential flow paths (Llopis-Albert
352 and Capilla, 2009). Moreover, as many authors have pointed out (e.g., Gómez-
353 Hernández and Wen, 1998), preferential flow pathways may play a crucial role for
354 tracer transport and may reflect some geological settings, e.g., channelling.
355 Eventually, for each one of the calibrated K fields obtained with the inverse model the
356 pollutant concentration response matrix is calculated, and the hydro-economic model
357 run.

358

359 **4. Results and discussion**

360 Fig. 3 shows the Cumulative Density Functions (CFD's) of the maximum benefits
361 obtained in the aquifer for both groundwater quality scenarios (S1 and S2) and both
362 conditional (to K and h data) and unconditional conductivity realizations (i.e., cases C1
363 and C2). Note that a forty year planning period is considered and a recovery time
364 horizon for the aquifer by the year 2015 has been defined, as established by the WFD.
365 As logical, this figure shows that when no groundwater quality restrictions are applied
366 in the optimization management model (i.e., for scenario S1) the same benefit is
367 obtained for all realizations and both cases, i.e., conditional and unconditional K fields.

368 Moreover, it represents the maximum benefit that can be achieved in the aquifer with
369 the defined set of parameters and variables. This is because farmers can applied as much
370 as fertilizer as required by each crop to maximize their yields as defined in Eq. (7).
371 Then, for scenario S1, the maximum benefit takes the value of 21.06 M€/year for all
372 realizations and both cases, so that the standard deviations of such CDF's are zero.
373 Contrary, for scenario S2, when groundwater quality constraints are applied (i.e.,
374 maximum nitrate concentrations of 50 mg/l are allowed at control wells) the benefits are
375 reduced for all realizations and both cases. As expected, for conditional K fields (C1)
376 and scenario S2, the uncertainty in the maximum benefits achieved in the aquifer is
377 strongly reduced if compared with the unconditional realizations (C2). In fact, the CDF
378 of the maximum benefits has a mean of 20.91 M€/year and a standard deviation of
379 0.074 M€/year for case C1, while it has a mean of 20.79 M€/year and a standard
380 deviation of 0.22 M€/year for case C2. This proves the worth of the methodology to
381 provide more reliable policies since it reduces the hydrogeological parameter
382 uncertainty, and therefore, the uncertainty in the decision variables of the management
383 model.

384 Similar results are obtained for the fertilizer applied to the aquifer as shown in Fig. 3. It
385 depicts the Cumulative Density Functions (CFD's) of the total fertilizer applied to the
386 aquifer for both groundwater quality scenarios and both conditional and unconditional
387 conductivity fields. Then, the maximum fertilizer applied to the aquifer is obtained for
388 S1. It has for both cases a mean of 3741.3 (ton/year) and a standard deviation of zero
389 For S2, case C1 has a mean of 3502.03 (ton/year) and a standard deviation of 129.51
390 (ton/year), while C2 takes the values of 3546.34 and 57.01, respectively. Again, there is
391 an important reduction in the uncertainty of the fertilizer applied to the aquifer.

392 Furthermore, the reduction of uncertainty is also depicted in Fig. 4, which shows the
393 breakthrough curves for control well #1 and scenario S2 (with groundwater quality
394 constraints of 50 mg/l) of all conditional conductivity realizations (C1). This figure
395 shows how close are the time series of nitrate concentrations of all conditional
396 realizations to the true K field. Note that these concentrations are restricted by the
397 management model to be lower, during the whole planning period, than the standard
398 enacted by the WFD.

399 The trade-offs between the economic returns and the reliability in meeting the
400 environmental standards can be compared for both scenarios. Fig. 2 and 3 show how the
401 scenario S1 leads to higher benefits than the scenario S2. Then higher nitrate
402 concentrations in the aquifer lead to lower benefits and vice versa. Therefore, these
403 trade-offs have been quantified under the WFD standards. Furthermore, they have been
404 quantified under an uncertain environment by means of the CDF of the agricultural
405 benefits and their respective nitrate concentrations.

406

407 **5. Conclusions**

408 In recent years, the concern about nitrate concentrations in groundwater has increased
409 on account of the intensive use of fertilizers in agriculture. Water legislations have dealt
410 with such issue by establishing limits of nitrate concentrations in groundwater bodies. In
411 Europe, the EU WFD establishes limits of 50 mg/l, and requires that groundwater
412 bodies reach a good quantitative and chemical status by 2015. Then to control
413 groundwater diffuse pollution is necessary to analyze and implement complex
414 management decisions. However, the decision-making process is even more complex
415 under uncertain environments and heterogeneous stakeholder's interests. This
416 uncertainty leads to different management policies with clear implications in reliability

417 levels, costs and benefits. Therefore policy-makers need agricultural advice services to
418 help them to come up with the best management practices. Such advices can be derived
419 from the results provided by the tool here presented, which entails the coupling of a
420 stochastic inverse model with a hydro-economic model. This allows reducing
421 uncertainty by constraining stochastic simulations to data. The stochastic hydro-
422 economic modeling framework has been verified in a 2D synthetic aquifer and its worth
423 for agricultural advice services demonstrated. It has been proved to be a valuable tool in
424 estimating non-Gaussian hydrogeological parameters such as the hydraulic conductivity
425 in highly heterogeneous aquifers. This leads to reducing uncertainty in concentration
426 distributions of contaminant plumes at control wells when reasonable amount of data is
427 available. Finally, this is translated into a reduction of the uncertainty on the results of
428 the hydro-economic model: maximum benefits, optimal strategies of spatial and
429 temporal allocation of fertilizer use in agriculture and concentrations in the aquifer that
430 meet certain groundwater quality standards. This has been carried out by means of a
431 sensitivity analyses for conditional and unconditional K fields. Furthermore, the trade-
432 offs between higher economic returns and reliability in meeting the environmental
433 standards have been analyzed for different groundwater quality scenarios. The study of
434 the least-cost alternative for meeting the environmental objectives is also important in
435 order to justify potential time and objective derogation when disproportionate costs are
436 identified (WFD, art. 4).

437 As a further research we could have considered different groundwater quality standards,
438 recovery time horizons, different spatial structure of the conductivity fields, or different
439 sets of flow and mass transport conditioning data (for instance, regarding the spatial
440 location and/or temporal).

441

442

443 **References**

444 - Bakr, M.I., te Stroet, C.B.M., Meijerink, A., 2003. Stochastic groundwater quality management: Role of
445 spatial variability and conditioning, *Water Resour. Res.*, 39(4), 1078, doi:10.1029/2002WR001745.

446 - Capilla, J.E., Llopis-Albert, C., 2009. Stochastic inverse modeling of non multiGaussian transmissivity
447 fields conditional to flow, mass transport and secondary data. 1 Theory. *Journal of Hydrology*, 371, 66-
448 74. doi:10.1016/j.jhydrol.2009.03.015.

449 - Deutsch, C.V., Journé, A.G., 1997. *GSLIB: Geostatistical Software Library and User's Guide*. New
450 York, Oxford University Press.

451 - Drud, A., 1985. CONOPT: a GRG code for large sparse dynamic nonlinear optimization problems.
452 *Math. Program.* 31, 153e191. doi:10.1007/BF02591747.

453 - EC, 1980. Council Directive 80/778/EEC relating to the quality of water intended for human
454 consumption. *Official Journal of the European Communities*, L229 (30.08.1980), pp. 11-29.

455 - EC, 2000. Directive 2000/60/EC of the European Parliament and of the Council of October 23 2000
456 Establishing a Framework for Community Action in the Field of Water Policy. *Official Journal of the*
457 *European Communities*, L327/1eL327/72. 22.12.2000.

458 - Gómez-Hernández, J.J., Srivastava, R.M., 1990. ISIM3D: An ANSI-C three dimensional multiple
459 indicator conditional simulation program. *Computer and Geosciences*, 16(4), 395-440.

460 - Gómez-Hernández, J.J., Wen, X.H., 1998. To be or not to be multiGaussian? A reflection on stochastic
461 hydrogeology. *Advances in Water Resources* 21 (1), 47-61.

462 - Hu, L.Y., 2000. Gradual deformation and iterative calibration of gaussian-related stochastic models.
463 *Mathematical Geology*, Vol. 32, No 1, 2000, 87-108.

464 - Neupauer, R.M., Wilson, J.L., 1999. Adjoint method for obtaining backward-in-time location and travel
465 time probabilities of a conservative groundwater contaminant. *Water Resources Research*, 35(11), 3389-
466 3398.

467 - Llopis-Albert, C., 2008. Stochastic inverse modelling in non-multiGaussian media conditional to flow,
468 mass transport and secondary data. PhD Thesis, Universitat Politècnica de València, 274 pp. ISBN: 978-
469 84-691-9796-7.

470 - Llopis-Albert, C., Capilla, J.E., 2009. Stochastic inverse modeling of non multiGaussian transmissivity
471 fields conditional to flow, mass transport and secondary data. 2 Demonstration on a synthetic aquifer.
472 *Journal of Hydrology*, 371, 53–65. doi:10.1016/j.jhydrol.2009.03.014.

473 - Llopis-Albert, C., Capilla, J.E., 2009a. Gradual conditioning of non-Gaussian transmissivity fields to
474 flow and mass transport data: 3. Application to the Macrodispersion Experiment(MADE-2) site, on
475 Columbus Air Force Base in Mississippi (USA). *Journal of Hydrology* 371, 75–84.
476 doi:10.1016/j.jhydrol.2009.03.016.

477 - Llopis-Albert, C., Capilla, J.E., 2010. Stochastic simulation of non-Gaussian 3D conductivity fields in a
478 fractured medium with multiple statistical populations: case study. *Journal of Hydrologic Engineering*,
479 15, 554-566. doi: 10.1061/(ASCE)HE.1943-5584.0000214.

480 - Llopis-Albert, C., Capilla, J.E., 2010a. Stochastic inverse modelling of hydraulic conductivity fields
481 taking into account independent stochastic structures: A 3D case study. *Journal of Hydrology* 391, 277–
482 288. doi:10.1016/j.jhydrol.2010.07.028.

483 - Llopis-Albert, C., Pulido-Velazquez, M., Peña-Haro, S., 2014. Assessment of the effect of uncertainty
484 on groundwater nitrate pollution control from agriculture. *Environmental Modelling & Software*,
485 submitted.

486 - McDonald, M.G., Harbough, A.W., 1988. A Modular Three-Dimensional Finite-Difference
487 Groundwater Flow Model, US Geological Survey Technical Manual of Water Resources Investigation,
488 Book 6, US Geological Survey, Reston, Va, 586 p.

489 - Peña-Haro S., Pulido-Velazquez, M., Sahuquillo, A., 2009. A hydro-economic modeling framework for
490 optimal management of groundwater nitrate pollution from agriculture. *Journal of Hydrology*, 373, 193–
491 203, doi:10.1016/j.jhydrol.2009.04.024.

492 - Peña-Haro, S., Llopis-Albert, C., Pulido-Velazquez, M, Pulido-Velazquez, D., 2010. Fertilizer standards
493 for controlling groundwater nitrate pollution from agriculture: El Salobral-Los Llanos case study, Spain.
494 *Journal of Hydrology*, 392, 174–187.

495 - Peña-Haro, S., Pulido-Velazquez, M., Llopis-Albert C., 2011. Stochastic hydro-economic modeling for
496 optimal management of agricultural groundwater nitrate pollution under hydraulic conductivity
497 uncertainty. *Environmental Modelling & Software* 26, 999-1008.

498 - Poeter, E.P., Hill, M.C., 1997. Inverse models: a necessary next step in ground-water modeling. *Ground*
499 *Water*;35(2):250–60.

500 - Rehfeldt, K.R., Boggs, J.M., Gelhar, L.W., 1992. Field study of dispersion in a heterogeneous aquifer 3.
501 Geostatistical analysis of hydraulic conductivity. *Water Resources Research*, 28(12), 3309–3324.

502 - Renard, P., 2007. Stochastic hydrogeology: what professionals really need? *Ground Water*, 45(5):531–
503 41. doi:10.1111/j.1745-6584.2007.00340.x.

504 - Salamon P., Fernández-García, D., Gómez-Hernández, J.J., 2006. Modeling mass transfer processes
505 using random walk particle tracking. *Water Resources Research*, 42, W11417,
506 doi:10.1029/2006WR004927.

507 - Smith, L., Schwartz, F.W., 1981. Mass transport, 2. Analysis of uncertainty in prediction. *Water*
508 *Resources Research*, 17(2):351–69.

509 - Williams, J.R., 1995. The EPIC model. In: Singh, V.P. (Ed.) *Computer Models of Watershed*
510 *Hydrology*, 909-1000. Water Resources Publisher.

511 - Zheng, C., Wang, P., 1999. MT3DMS: A Modular Three-Dimensional Multispecies Transport Model
512 for Simulation of Advection, Dispersion and Chemical Reactions of Contaminants in Groundwater
513 Systems; Documentation and User's Guide.

514

515

516

517

518

519

520

521

522

523

524

525

526 Table 1. Sources, crops and irrigation.

527

Source	Crop	Area (ha)	Water applied (m³/ha)	Crop price (€/kg)
S1	Alfalfa	3600	950	0.09
S2	Barley	3600	300	0.12
S3	Sunflower	3600	400	0.30
S4	Wheat	3600	250	0.13
S5	Corn	3600	700	0.12

528

529

Figure1

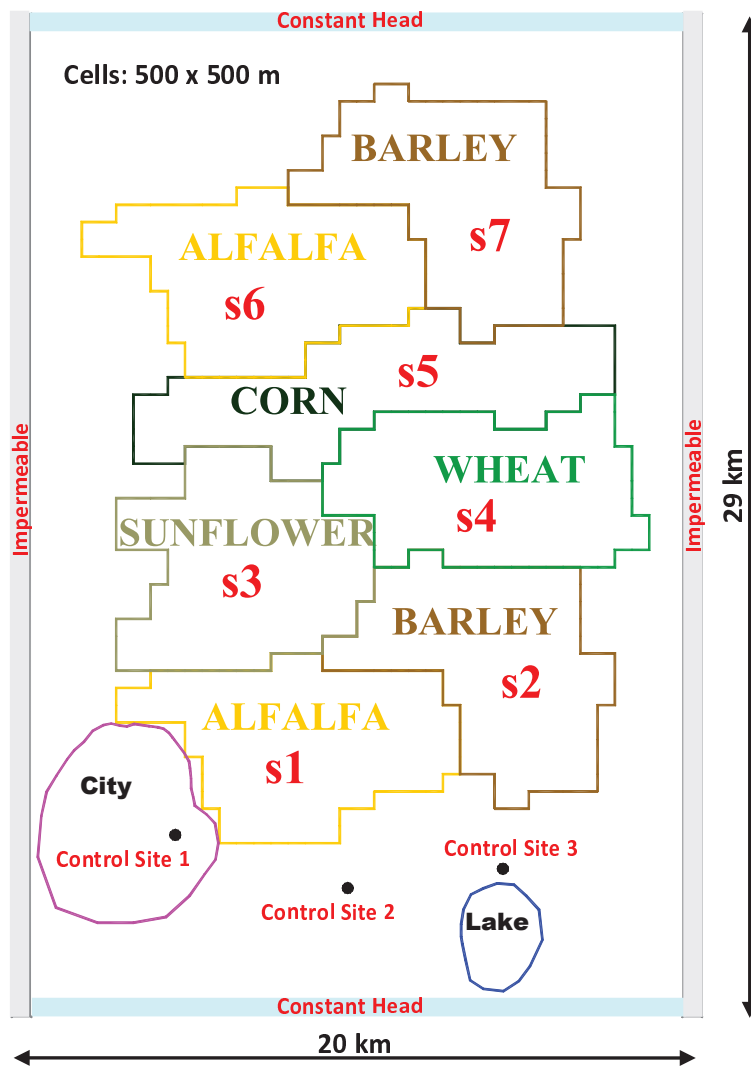


Figure2

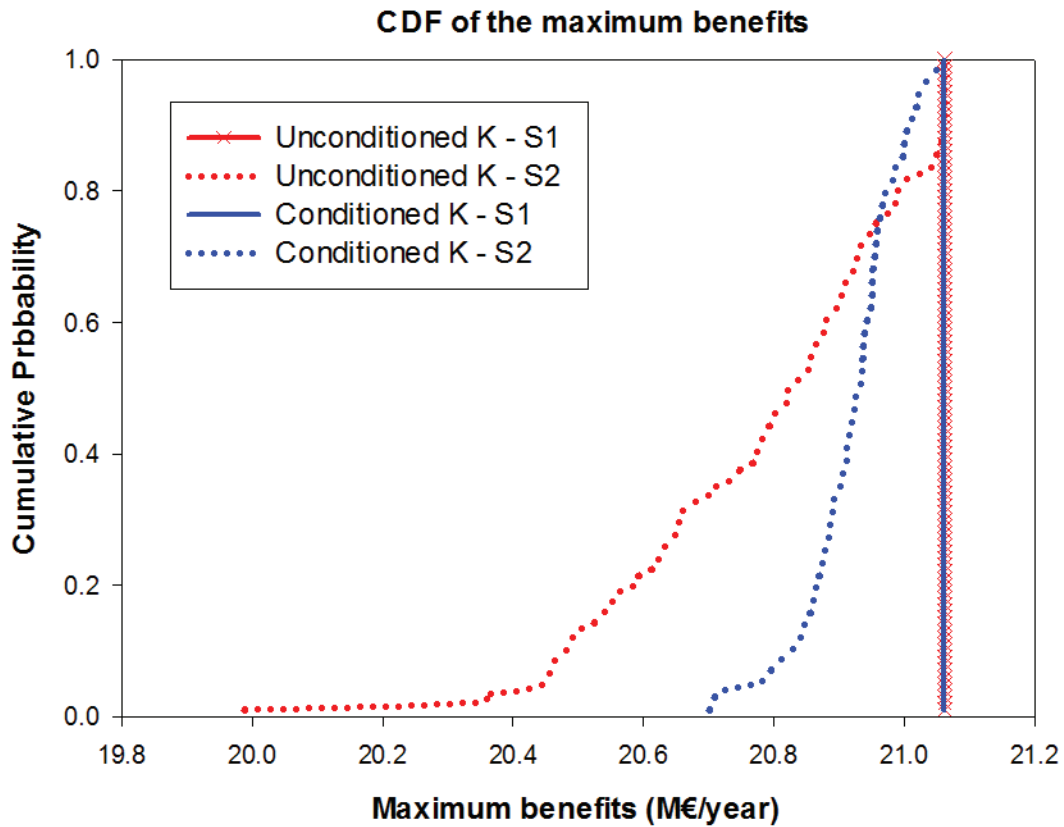


Figure3

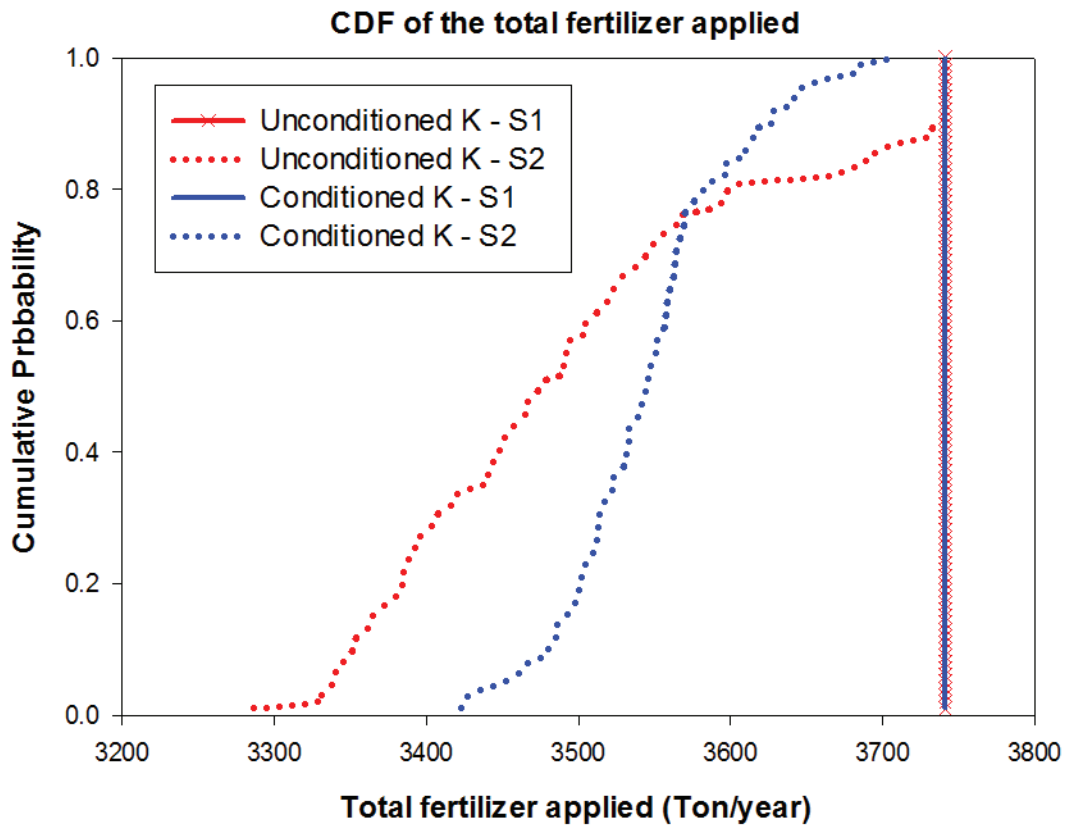


Figure4

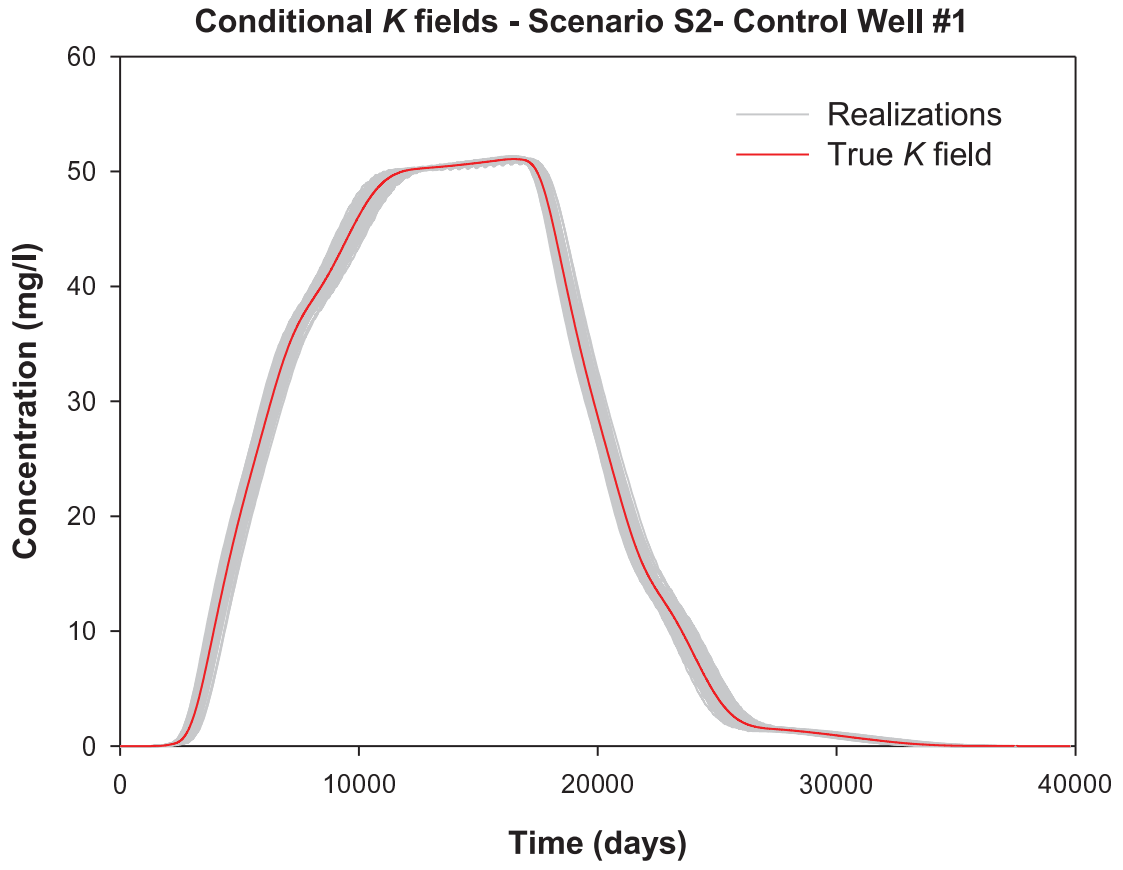


Figure Captions

Figure 1. Problem domain, boundary conditions, control areas (s_i) and crops and spatial location of the observation sites.

Figure 2. Cumulative Density Functions (CFD's) of the maximum benefits (M€/year) for both groundwater quality scenarios and both conditional and unconditional conductivity fields.

Figure 3. Cumulative Density Functions (CFD's) of the total fertilizer applied to the aquifer (Ton/year) for both groundwater quality scenarios and both conditional and unconditional conductivity fields.

Figure 4. Breakthrough curves for control well #1 and scenario S2 (groundwater quality constraints of 50 mg/l) of the conditional conductivity fields. The figure also shows the true field. A planning period of forty years is considered.